ACS Catalysis

Research Article

pubs.acs.org/acscatalysis

Efficient Room-Temperature Aqueous-Phase Hydrogenation of Phenol to Cyclohexanone Catalyzed by Pd Nanoparticles Supported on Mesoporous MMT-1 Silica with Unevenly Distributed Functionalities

Chi-Jui Lin,[†] Shao-Hsien Huang,[†] Nien-Chu Lai,[†] and Chia-Min Yang*[,†,‡]

[†]Department of Chemistry and [‡]Frontier Research Center on Fundamental and Applied Sciences of Matters, National Tsing Hua University, Hsinchu 30013, Taiwan

Supporting Information

ABSTRACT: Efficient and selective aqueous-phase hydrogenation of phenol by a novel Pd catalyst supported on dually and selectively functionalized mesoporous MMT-1 silica nanoparticles has been developed. The catalyst features small (~1.1 nm) Pd nanoparticles surrounded by unevenly distributed nitrogen- or heteroatom-free organic groups in the helical mesopores and the presence of non-hydrogen-bonded isolated silanol groups on the mesopore surface. The catalyst exhibited superior conversion of phenol and high selectivity of cyclohexanone at room temperature under atmospheric pressure of hydrogen and remained highly active after ten catalytic runs. The catalyst was active for the aqueous-phase hydrogenation of a variety of mono- and dihydroxylated aromatic compounds. The green protocol with the designed catalyst would be practical for the hydrogenation of phenol and other derivatives.

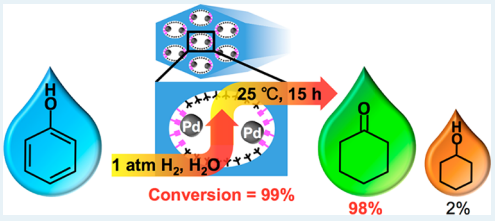

KEYWORDS: *supported palladium catalyst, mesoporous silica, unevenly distributed functionalities, phenol hydrogenation, room-temperature aqueous-phase reaction*

1. INTRODUCTION

Cyclohexanone is of great industrial importance and is utilized as an intermediate in the production of caprolactam and adipic acid for fabricating nylon-6, nylon-66, and polyamide resins.[1−3] Industrially, cyclohexanone can be produced either by the oxidation of cyclohexane[4−6] or via the hydrogenation of phenol.[7−31] The oxidation of cyclohexane requires high temperatures and high pressures and suffers from low product yields and complicated recovery/separation steps.[4−6] On the other hand, the hydrogenation of phenol to cyclohexanone may take place in one-step (direct) fashion or via the formation of cyclohexanol followed by dehydrogenation (two-step process).[18,19,32] The one-step and selective hydrogenation of phenol is certainly greener and therefore preferable, but cyclohexanone is rather active and may be easily further hydrogenated to cyclohexanol or other byproducts.[7,13,17] Hence, it remains crucial and challenging to develop effective catalysts for the reaction.

Phenol hydrogenation can be catalyzed by a variety of supported Pd catalysts.[7−24,26−29] Traditionally, the reaction has been conducted in the gas phase at high temperatures, but it often suffers from catalyst deactivation due to coking.[7−13,15,16] Numerous recent studies focused on the development of new types of Pd catalysts for the liquid-phase phenol hydrogenation at relatively low temperatures.[14,17−31] A remarkable example was reported by Han and co-workers showing high phenol conversion and high cyclohexanone selectivity for the reaction catalyzed by a dual-supported Pd Lewis acid catalyst in dichloromethane at 50 °C and 10 atm of H_2.[20] However, the presence of Lewis acid imposes severe limitations on the use of the catalyst in hydrogenation reactions, and the reaction conditions are not environmentally friendly. It is highly desired if the reaction could proceed under atmospheric pressure of H_2 in a green solvent, such as water. Camaioni, Lercher, and their co-workers applied X-ray absorption spectroscopy and showed that the state of supported zero-valence Pd nanoparticles (NPs) in contact with H_2 in the aqueous phase remains unchanged during hydrogenation reactions.[33] To date, very few Pd catalysts comprising metallic NPs that are either stabilized in polymers[25,31] or dispersed on mesoporous nitrogen-containing carbons,[24,27−29] polymer-functionalized carbon nanotubes,[26] and metal−organic framework MIL-101[22] have been reported to be capable of catalyzing aqueous-phase phenol hydrogenation. For the MIL-101-supported catalyst, there is concern on possible release of hazardous chromium ions in aqueous conditions. On the other hand, while the presence of nitrogen-bearing groups or moieties is essential for polymer- or carbon-based supports to adsorb ionic Pd precursors and achieve high metal dispersion, problems of particle detachment and metal leaching[27] are often encountered. There remains great need to develop highly efficient, selective and stable catalysts for the green hydrogenation process.

Received: February 19, 2015
Revised: May 10, 2015

DOI: 10.1021/acscatal.5b00380
ACS Catal. 2015, 5, 4121−4129

We herein report a novel Pd catalyst supported on functional mesoporous silica NPs for room-temperature aqueous-phase hydrogenation of phenol to cyclohexanone. Mesoporous silicas are highly attractive supports for metal NPs because of their chemical stability, high surface area, and versatile chemistry of surface functionalization. We have recently developed a new type of mesoporous silica nanostructures, designated as MMT-1, that features low-symmetry 2D-rectangular mesostructure and elliptical (instead of cylindrical) and helical channels resulting from microphase segregation of structure-directing cationic and nonionic surfactants.[34−37] Aiming at nonconventional supports[38−40] for highly active and recyclable Pd catalysts, as shown in Scheme 1, we constructed unevenly functionalized MMT-1 by selective surfactant extraction, sequential modification of trimethylsilyl and trivinylsilyl groups, and finally Pd deposition. The catalyst features small size of Pd NPs in the helical channels, purely hydrocarbon-containing (free from nitrogen or other heteroatoms) groups unevenly surrounding Pd NPs and the presence of isolated silanol groups on mesopore surface. The catalyst exhibited superior conversion of phenol (99%) and high selectivity of cyclohexanone (98%) at 1 atm H_2 and 25 °C, and it remained highly active even after ten reuse cycles. Furthermore, the catalyst could also catalyze selective partial hydrogenation of a variety of phenol derivatives under mild conditions. The efficient and recyclable catalyst is believed to be active for the hydrogenation of other phenol derivatives.

Scheme 1. Schematic Representation of the Preparation of Pd@sMMT-1 by Selective Surfactant Extraction, Sequential Surface Modification, and Pd Deposition

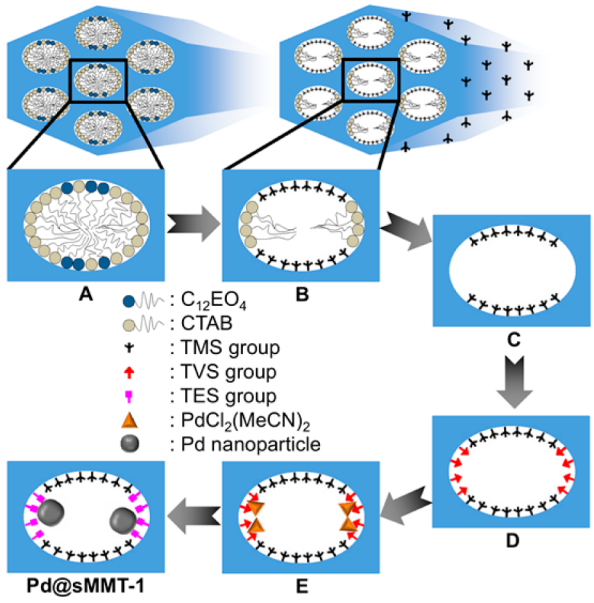

2. EXPERIMENTAL SECTION

2.1. Catalyst Preparation. Mesoporous MMT-1 silica was synthesized by following the reported procedure[34,35] using tetramethoxysilane (TMOS) as a silica source, sodium hydroxide (NaOH) as a base, cetyltrimethylammonium bromide (CTAB), and tetraethylene glycol dodecyl ether ($C_{12}EO_4$) as structure-directing agents. The molar composition of the synthesis mixture was 8 TMOS:0.30 $C_{12}EO_4$:0.70 CTAB:2.56 NaOH:9600 H_2O. The mixture was aged at 90 °C for 24 h, and the as-synthesized MMT-1 (Sample **A** in Scheme 1) was filtered and dried. Sample **A** (1.0 g) was stirred in a mixture of chloroform (10 mL) and hexamethyldisilazane (HMDS, 2 mL) at 35 °C for 24 h to preferentially extract $C_{12}EO_4$ from the sample and at the same time modify the exposed surface with trimethylsilyl (TMS) groups (sample **B**). For the purpose of comparison, pure chloroform instead of mixture with HMDS was used to treat sample **A** to result in sample **B′**. To remove the remaining CTAB, sample **B** (1.0 g) was stirred in ethanol solution (C_2H_5OH, 150 mL) of ammonium nitrate (NH_4NO_3, 0.3 g) at 50 °C[41] and was then repeatedly washed by C_2H_5OH and finally dried at 150 °C under vacuum (sample **C**). Sample **C** (1.0 g) was stirred in toluene (20 mL) solution of trivinylchlorosilane (TVCS, 5 mL) at 50 °C for 8 h to graft trivinylsilyl (TVS) groups onto the mesopore surface that were not modified with TMS groups. The dually and selectively functionalized MMT-1 (denoted as sMMT-1, sample **D**) was washed with toluene and acetone and was finally dried under ambient conditions. For the incorporation of Pd, sample **D** (0.2 g) was stirred in dichloromethane solution (10 mL) of bis(acetonitrile)-dichloropalladium(II) ($PdCl_2(MeCN)_2$, 0.042 g) for minutes and the colored solid (sample **E**) was washed by dichloromethane and dried in ambient. The metal was reduced in flowing H_2 at 100 °C for 3 h to obtain the sample Pd@sMMT-1.

Two MMT-1-supported Pd samples were also prepared as references for the study. The first sample used dually but randomly functionalized MMT-1 (denoted as rMMT-1) as a support for Pd deposition by following the same procedure as that for Pd@sMMT-1. For the preparation of rMMT-1, the as-synthesized MMT-1 (sample **A**, 1.0 g) was stirred in toluene solution (20 mL) of HMDS (2 mL) at 35 °C for 2 h to modify the external surface with TMS groups, stirred in the C_2H_5OH solution (150 mL) of NH_4NO_3 (0.3 g) at 50 °C to remove all the surfactants,[41] and finally stirred in toluene solution (20 mL) containing TVCS (4.4 mL) and trimethylchlorosilane (TMCS, 0.6 mL) at 50 °C for 8 h to graft TMS and TVS groups simultaneously on the mesopore surface of MMT-1. In the final step, TMCS instead of HMDS was used because of its compatibility with TVCS. Besides, both TMCS and TVCS generate the same byproduct of hydrogen chloride (instead of ammonia for HMDS) after the reaction with surface silanols and water. The doses of TVCS and TMCS used were varied and tested in order to result in rMMT-1 with the same relative amounts of TVS and TMS groups with those in sMMT-1. The other reference sample, denoted as Pd@MMT-1-IMP, was prepared by using the externally TMS-modified MMT-1 as a support to load $PdCl_2(MeCN)_2$ by incipient wetness impregnation (with dichloromethane as a solvent) followed by the reduction process in H_2 flow. The metal loading was kept the same with that for Pd@sMMT-1 and Pd@rMMT-1.

2.2. Catalyst Characterization. Powder X-ray diffraction (PXRD) data were obtained on a Mac Science 18MPX diffractometer using Cu Kα radiation. N_2 physisorption isotherms were measured at 77 K using a Quantachrome Autosorb-1-MP instrument. The isotherms were analyzed by the nonlocal density functional theory (NLDFT) method to evaluate pore sizes using the kernel of NLDFT equilibrium capillary condensation isotherms of N_2 at 77 K on silica (adsorption branch, assuming cylindrical pore geometry). BET surface areas were calculated from adsorption branches in the relative pressure range of 0.05−0.20. Total pore volumes were

DOI: 10.1021/acscatal.5b00380
ACS Catal. 2015, 5, 4121−4129

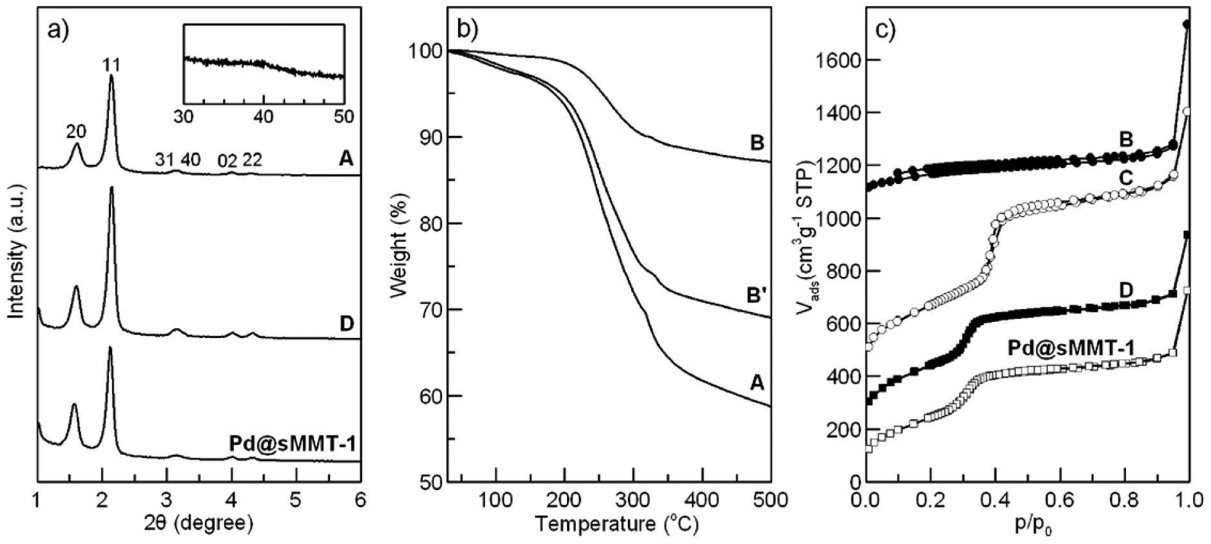

Figure 1. Small-angle PXRD patterns (a), TG data (b), and N_2 physisorption isotherms (c) of selected samples. (a, inset) Wide-angle pattern of Pd@sMMT-1. The isotherms are shifted (from bottom to top) by 0, 200, 300, and 1100 cm^3 g^{-1} STP, respectively.

evaluated at a relative pressure of 0.95. Liquid-state ^{13}C NMR spectra were measured on a Varian Unity Inova 500 MHz NMR spectrometer. Solid-state ^{29}Si and ^{1}H MAS NMR spectra were measured on a Bruker Avance III 400 MHz NMR spectrometer using 4 mm MAS probe. Thermogravimetry (TG) data were obtained using a Linseis STA PT1600 device. Elemental analysis (EA) data were obtained using a Elementar Vario EL III device. X-ray photoelectron spectroscopy (XPS) data were obtained using a Ulvac-PHI PHI Quantera device. Inductively coupled plasma-mass spectroscopy (ICP-MS) data were obtained using a Agilent 7500ce device. Transmission electron microscopy (TEM) and scanning transmission electron microscopy (STEM) images were taken from ultramicrotomed samples (thickness of 80−100 nm, supported on carbon-coated copper grids) by using a field-emission microscope operated at 200 keV (FEI F20 G2) with an electron-probe size of ∼2 Å and equipped with a high-angle annular dark-field (HAADF) detector and an energy-dispersive X-ray spectrometer (EDX). X-ray absorption spectroscopy (XAS) measurements at the Pd K-edge (24350 eV) were carried out in the transmission mode on the beamline 01C1 of the National Synchrotron Radiation Research Center (NSRRC, Taiwan) with a storage ring energy of 1.5 GeV. A powdery sample (24 mg) was pressed to form a wafer to be mounted in an in situ cell. The sample was heated in H_2 at 100 °C for 1 h and was then cooled to 25 °C for the measurements. Extended X-ray absorption fine structure (EXAFS) spectra were recorded for structural analysis. Multiple scans were averaged to improve the signal-to-noise ratio.

2.3. Catalytic Studies on the Hydrogenation of Phenol. A Pd catalyst was placed into a 20 mL Schlenk flask equipped with a magnetic bar. The system was evacuated (5×10^{-3} Torr) before being purged with H_2 (99.999%). The catalyst was activated by heating at 100 °C under H_2 for 1 h before adding water and phenol into the flask. The reaction mixture contained phenol (0.50 mmol), water (2.0 mL), and a Pd catalyst (0.15−1.5 mol % of Pd relative to phenol), and the reaction was stirred (at ∼800 rpm) and conducted at 25−35 °C under 1 atm of H_2 for 5−15 h. H_2 was continuously supplied to maintain the pressure during the reaction. After the reaction, the mixture was extracted with ethyl acetate and the products (added with *n*-hexadecane as an internal standard) were analyzed by a Shimadzu GC-2014 equipped with a FID detector and a SolGel-WAX column. In addition to Pd@sMMT-1, Pd@rMMT-1, Pd@MMT-1-IMP, and a commercial carbon-supported Pd (Pd/C, 5 wt %, Alfa Aesar, containing ∼10 nm Pd particles after reduction) were used to catalyze the reaction. For the reuse tests, the catalysts were collected by centrifugation, dried, and then reused in next runs. To examine the substrate scope, a variety of phenol derivatives were used as received for the hydrogenation reaction at 25−65 °C under 1 atm of H_2 for 15 h.

3. RESULTS AND DISCUSSION

The as-synthesized MMT-1 silica had highly ordered 2D-rectangular (with *c2mm* symmetry) mesostructure, as indicated by the small-angle PXRD pattern of sample **A** in Figure 1a showing intense 20, 11, and other high-order reflections. The derived cell parameters *a* and *b* were 11.0 and 4.5 nm, respectively. The structural order and the unit cell dimension remained unchanged after subsequent treatments, modifications, and metal deposition (cf. Figure 1a). Sample **A** contained ∼25.2 wt % surfactants, as suggested by the weight loss between 220 and 340 °C during TG analysis (Figure 1b). EA data of the surfactant mixture obtained by complete extraction in C_2H_5OH solution of NH_4NO_3 at 50 °C further indicated that the molar ratio of CTAB and $C_{12}EO_4$ in **A** was 76:24, which is close to the nominal value of the synthesis mixture (70:30). The weight percentages of CTAB and $C_{12}EO_4$ in **A**, as derived from combining TG and EA data, were 19.2 and 6.0 wt %, respectively. When the sample was extracted with chloroform to result in sample **B′**, the surfactants extract contained 0.7 wt % of CTAB and 5.2 wt % of $C_{12}EO_4$, as revealed by EA and ^{13}C NMR (Figure S1, determined by taking the intensity ratio of the lines corresponding to —N($\underline{C}H_3)_3^+$ of CTAB and —$\underline{C}H_2OH$ of $C_{12}EO_4$). The preferential (and almost complete) extraction of $C_{12}EO_4$ by chloroform took place owing to weak interactions between the nonionic surfactant and (partially) anionic silica wall.[34,35] Alternatively, the extraction was performed in the mixture of chloroform and HMDS in order to simultaneously modify the exposed silica surface with TMS groups (resulting in sample **B**). HMDS instead TMCS

DOI: 10.1021/acscatal.5b00380
ACS Catal. 2015, 5, 4121−4129

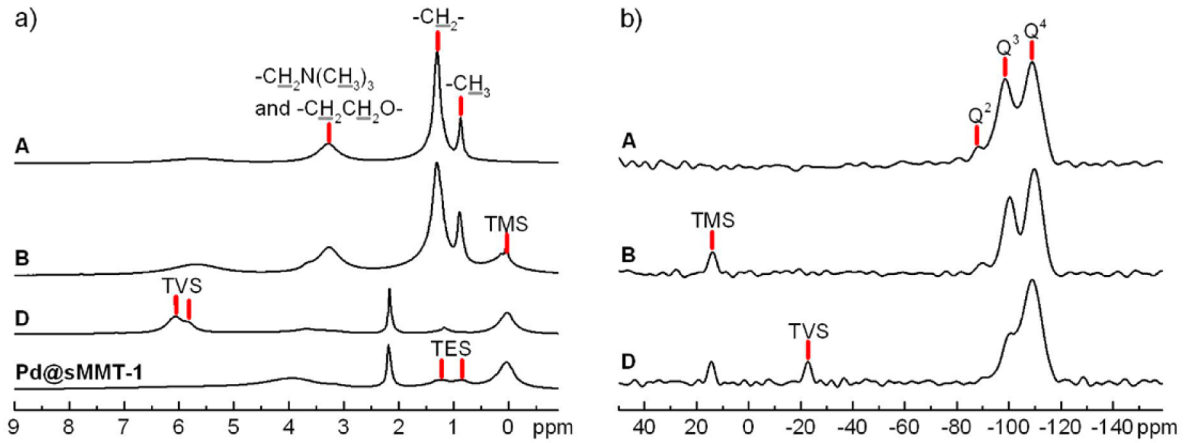

Figure 2. Solid-state ^{1}H (a) and ^{29}Si (b) MAS NMR spectra of selected samples.

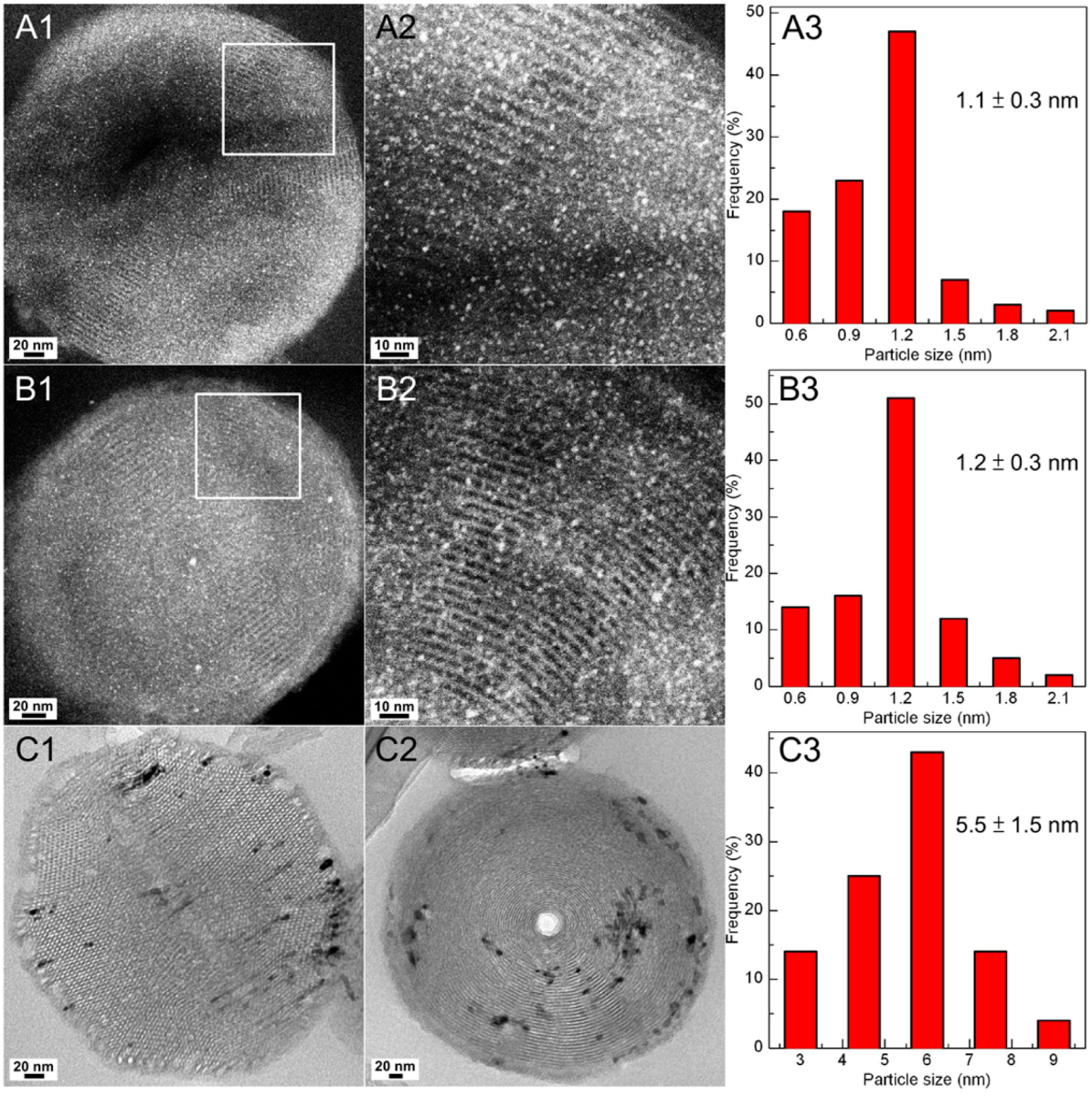

Figure 3. (A and B) STEM-HAADF images (with the magnified images shown in A2 and B2) and the corresponding particle size distribution of Pd@sMMT-1 (A3) and Pd@rMMT-1 (B3). (C) TEM images and particle size distribution of Pd@MMT-1-IMP.

DOI: 10.1021/acscatal.5b00380
ACS Catal. 2015, 5, 4121−4129

was used because the reaction of TMCS with surface silanols and water generates hydrogen chloride as a byproduct that may facilitate the extraction of CTAB by ion exchange and fail the preferential extraction of $C_{12}EO_4$. Results of EA and ^{13}C NMR (Figure S1) indicated that the surfactants extract consisted of 11.4 wt % of CTAB and 5.4 wt % of $C_{12}EO_4$. Obviously, the extraction with HMDS removed not only all $C_{12}EO_4$ but also ~59% of the CTAB from the as-synthesized sample, which could be attributed to the ion exchange of CTAB with the ammonia molecules generated from the reactions of HMDS with surface silanol (Si−OH) groups and residual water.

The simultaneous modification of sample **B** was confirmed by solid-state NMR. As shown in Figure 2a, while the ^1H MAS NMR spectrum of **A** shows lines attributed to the protons of CTAB and $C_{12}EO_4$, the spectrum of **B** contains an additional line at 0 ppm that can be assigned to the protons of TMS groups. ^{29}Si MAS NMR (Figure 2b) revealed that the modification was accompanied by the consumption of silanol groups, and quantitative analysis suggested the relative amounts of different silicon species to be Q^2:Q^3:Q^4 = 5:42:53 for **A** and TMS:Q^2:Q^3:Q^4 = 6:5:36:59 (or TMS:Q^n = 6:100) for **B** (Q^n:$Si(OSi)_n(OH)_{4-n}$, n = 2, 3, 4). The sample **B** still contained significant amount of CTAB and did not possessed noticeable mesoporosity, as suggested by N_2 physisorption analysis (cf. Figure 1c). The remaining surfactant could be removed completely by further extraction in C_2H_5OH solution of NH_4NO_3, and the resulting sample **C** exhibited type IV isotherm with a step at the relative pressure of ~0.4, indicative of the presence of channel-type mesopores with a diameter of 4.4 nm. The BET surface area and total pore volume of **C** are 1092 $m^2\ g^{-1}$ and 1.06 $cm^3\ g^{-1}$, respectively.

After further grafting with TVS groups, the resulting sample **D** exhibited decreased mesopore size of 3.8 nm, surface area of 971 $m^2\ g^{-1}$, and total pore volume of 0.89 $cm^3\ g^{-1}$. The TVS groups gave rise to additional lines in the ^1H spectrum at 5.8 and 6.1 ppm, and the relative amounts of TVS, TMS, and Q^n species were estimated to be 6:6:100 by ^{29}Si MAS NMR (cf. Figure 2). Notably, in the ^1H spectrum of **D**, there appeared a narrow peak at 2.2 ppm which may be attributed to the non-hydrogen-bonded isolated silanol groups on the surface of MMT-1 according to the solid-state NMR study on similar type of materials (MCM-41 silica) by Pruski and co-workers.[42] Such surface species are rarely observed on pure-silica, TMS-functionalized, or organically functionalized mesoporous silicas.[42−44] To examine if the presence of the isolated silanol groups is associated with the spatially selective dual functionalization, we prepared a sample with randomly distributed TMS and TVS groups (i.e., the sample denoted as rMMT-1) by reacting the surfactant-free MMT-1 simultaneously with controlled amounts of TMCS and TVCS (see the Experimental Section for details). As shown in Figure S2, with nearly identical relative amounts of TMS and TVS groups to those for **D**, rMMT-1 did not exhibit discernible peak at 2.2 ppm in its ^1H MAS NMR spectrum. The results reveal the uniqueness of the spatially arranged chemical environment of the nanospace in sample **D**. As for the location of those isolated silanol groups in **D**, they are most likely to be present in between TVS groups that are slightly bulkier than TMS groups and might prevent the reaction between the isolated silanol groups and TVCS during the process of secondary modification.

The incorporation of Pd NPs was accomplished by reacting **D** with $PdCl_2(MeCN)_2$ followed by reduction in H_2 flow at 100 °C. The Pd^{2+} species were anchored in the samples by forming π-bonded complexes with the vinyl moieties of TVS groups,[38,45] and they were completely reduced by H_2 to form metallic Pd NPs as confirmed by XPS (Figure S3). Quantitative analyses of EDX and ICP-MS showed that, based on the weights of silica and Pd, the metal loading of the resulting sample Pd@sMMT-1 was 6.2 wt %. It was noted that the H_2 treatment also transformed TVS groups to triethylsilyl (TES) groups, probably through Pd-catalyzed hydrogenation, and that gave rise to the lines at 0.8 and 1.2 ppm accompanied by the disappearance of the lines attributed to TVS groups in the ^1H MAS NMR spectrum of Pd@sMMT-1 (cf. Figure 2a). Despite having relatively high metal loading, Pd@sMMT-1 exhibited very broad reflections of the metal in its wide-angle PXRD pattern (cf. Figure 1a) and gave a N_2 physisorption isotherm showing no sign of pore blocking (cf. Figure 1c). The results strongly suggested that the reduced Pd formed very small NPs in the functionalized MMT-1. STEM investigation further provided direct evidence. As shown in Figure 3A, STEM-HAADF images clearly show that Pd NPs with average size of ~1.1 nm are highly dispersed in the channels of MMT-1. We also estimated the average particle size of Pd NPs in the reduced Pd@sMMT-1 by XAS. The Fourier transform (FT) profiles of the k^3-weighted EXAFS data and the curve fitting results are shown in Figure S4. The coordination number of Pd−Pd shell was 7.1, and the Pd particle size are estimated to be around 1.1 nm based on a face-centered cubic structure of Pd and a spherical model.[46] Figure 3 also compares the TEM images of the two reference samples Pd@rMMT-1 and Pd@MMT-1-IMP. Pd@rMMT-1 was prepared with rMMT-1 by the same route of Pd incorporation as for Pd@sMMT-1, and the metal loading was the same (6.2 wt %) as that for Pd@sMMT-1. As mentioned in the Experimental Section, Pd@MMT-1-IMP was prepared by incipient wetness impregnation of calculated amount of $PdCl_2(MeCN)_2$ followed by H_2 reduction to result in the same Pd loading of 6.2 wt %. Similar situation of high metal dispersion was found in Pd@rMMT-1, whereas Pd NPs and nanorods extended along the mesopores of MMT-1 were clearly observed in Pd@MMT-1-IMP (Figure 3C). Results of wide-angle PXRD analyses (Figure S5) were consistent with the TEM observation. To further show the crucial role of TVS for achieving high metal dispersion, we also used sMMT-1 to load the same amount (6.2 wt %) of Pd NPs by incipient wetness impregnation of $PdCl_2(MeCN)_2$ (followed by H_2 reduction) and similar degree of metal dispersion and average particle size (~1.2 nm) were observed for this sample (cf. Figure S6). Obviously, the formation of highly dispersed Pd NPs is mainly associated with the coexistence of TMS and the Pd^{2+}-anchoring TVS groups, both of which have to be distributed (either unevenly or randomly) along the channel-type mesopores.

The MMT-1-supported Pd catalysts and commercial Pd/C were activated and applied for the aqueous-phase hydrogenation of phenol, and the results are shown in Table 1. Prior studies have shown that Pd catalyst is capable of hydrogenating the benzene ring of phenol to produce 1-cyclohexenol that is unstable and transform rapidly to cyclohexanone via tautomerization and cyclohexanone can then be further hydrogenated by Pd to form cyclohexanol as main product (Scheme 2).[7−24,26−29] When Pd@sMMT-1 (1.5 mol % Pd relative to phenol) was applied as a catalyst, a phenol conversion of 70% and a cyclohexanone selectivity of 99% were obtained at 35 °C with a reaction time of 5 h (entry 1). The conversion was

DOI: 10.1021/acscatal.5b00380
ACS Catal. 2015, 5, 4121−4129

Table 1. Aqueous-Phase Phenol Hydrogenation with Pd Catalysts[a]

entry	catalyst	Pd amount (mol %)	T (°C)	time (h)	conversion (%)	selectivity[b] (%) CH-one	CH-ol
1	Pd@sMMT-1	1.5	35	5	70	99	1
2	Pd@sMMT-1	1.5	35	10	95	99	1
3	Pd@sMMT-1	1.5	35	15	>99	98	2
4[c]	Pd@sMMT-1	1.5	35	15	>99	69	31
5	Pd@sMMT-1	1.5	25	5	65	99	1
6	Pd@sMMT-1	1.5	25	15	99	98	2
7	Pd@sMMT-1	0.3	25	15	74	99	1
8	Pd@sMMT-1	0.15	25	15	69	99	1
9	Pd@rMMT-1	1.5	25	5	57	99	1
10	Pd@rMMT-1	1.5	25	15	85	98	2
11	Pd@MMT-1-IMP	1.5	25	15	45	96	4
12	Pd/C	1.5	25	15	43	85	15

[a]The reactions were carried out using phenol (0.5 mmol), a Pd catalyst (0.15−1.5 mol % of Pd relative to phenol), and water (2.0 mL) in H_2 (1 atm) at 25−35 °C for 5−15 h. [b]CH-one and CH-ol denote cyclohexanone and cyclohexanol, respectively. [c]The non-activated catalyst was used.

Scheme 2. Phenol Hydrogenation over Pd Catalyst

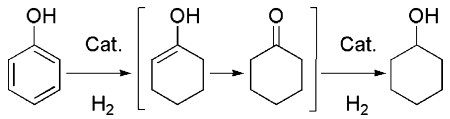

increased when prolonging the reaction time, and nearly all the reactant was consumed after reacting for 15 h while the selectivity was almost the same (entries 2 and 3). Notably, the selectivity of cyclohexanone was greatly influenced by the step of H_2 activation, and the value decreased to 69% for the reaction with nonactivated catalyst at 35 °C for 15 h (entry 4). Since the activation process reduced surface oxide (e.g., PdO) formed when the reduced Pd NPs were exposed to air, the results seem to suggest that the surface oxide species might facilitate further hydrogenation of cyclohexanone to form cyclohexanol under the reaction conditions of 1 atm H_2 at 35 °C in aqueous medium. The performance of Pd@sMMT-1 at 25 °C was almost the same with that at 35 °C (entries 5 and 6), making the sample superior and highly selective catalyst for room-temperature aqueous-phase hydrogenation of phenol to cyclohexanone. Noticeably, the usage of Pd@sMMT-1 could be markedly reduced from 1.5 mol % to 0.15 mol % with decent phenol conversion (entries 7 and 8), making the "green" catalytic system more attractive for practical applications. We further conducted reactions using the conditions for entry 5 except the amount of water (1.0 and 5.0 mL) to study the influence of phenol concentration on its conversion. We found that the conversion only changed slightly (61% and 67% for 0.1 and 0.5 M phenol, respectively), suggesting the absence of mass transfer limitations under the reaction conditions.

On the other hand, Pd@rMMT-1 with randomly distributed surface groups was also highly active and selective for the reaction and exhibited lower phenol conversion than Pd@sMMT-1 did under the same reaction conditions (entries 9 and 10). For comparison, the reference catalyst Pd@MMT-1-IMP showed much lower (45%) phenol conversion but fair cyclohexanone selectivity after reacting for 15 h (entry 11), and the commercial Pd/C exhibited lower conversion and poorer selectivity (entry 12) than all the MMT-1-supported Pd catalysts. The impressive catalytic performance of Pd@sMMT-1 and Pd@rMMT-1 should be mainly attributed to the small size of the Pd NPs in the samples. It is known that phenol tends to adsorb from water onto hydrophobic adsorbents such as carbon materials.[47] Besides, the solubility of H_2 in nonpolar solvents is generally larger than that in water, especially when the solvent is geometrically confined to a few nanometers.[48] The presence of the hydrophobic TMS and TES groups on the mesopores may also be beneficial for the concentration of the reactants (i.e., phenol and H_2) into the catalysts. Moreover, the fact that Pd@sMMT-1 showed even higher phenol conversion than Pd@rMMT-1 may be associated with the distinct chemical environment surrounding the Pd NPs. Regarding the high selectivity of cyclohexanone, it is generally accepted that the product selectivity is mainly associated with the orientation (or geometry) of the phenol molecules adsorbed on the catalyst surface: The coplanar phenol adsorption is favorable for saturated hydrogenation to produce cyclohexanol, while the nonplanar adsorption generally leads to partial hydrogenation to cyclohexanone.[17,24] For the reactions catalyzed by the reduced Pd@sMMT-1 and Pd@rMMT-1, phenol molecules may interact relatively strongly with the surface (through hydrogen bonding to silanol groups) to result in nonplanar adsorption. The benzene ring of phenol may then be partially hydrogenated to the enol, which can rapidly isomerize to give cyclohexanone. Since cyclohexanone interacts weakly to the surface, it leaves the catalytic site quickly and is replaced by a more strongly binding phenol molecule, avoiding further hydrogenation to cyclohexanol. As mentioned before, there existed the non-hydrogen-bonded isolated silanol groups on the mesopore of Pd@sMMT-1 (or sample **D** before Pd incorporation) and they were most likely to be located in between TES groups (or TVS groups before Pd incorporation). As shown in Scheme 3, we speculated that the isolated silanol groups in Pd@sMMT-1 might interact with phenol molecules through hydrogen bonding[49] and orient the benzene ring of these molecules toward the neighboring Pd NPs, thereby facilitating the hydrogenation process. Such an effect might be absent or less pronounced for Pd@rMMT-1, in which the nonisolated silanol groups would mainly form hydrogen bonds with water or adjacent silanol groups.

The reuse tests of Pd@sMMT-1 (1.5 mol % Pd) for the aqueous-phase phenol hydrogenation at room temperature (25 °C) were conducted. After each reaction, the catalyst was collected by centrifugation, drying and then reused in the next run. As shown in Figure 4, Pd@sMMT-1 was highly reusable and the conversion of phenol only dropped slightly from 99% for the first run to 73% for the tenth run with the selectivity of cyclohexanone unchanged (98%). The reasons for the slight decrease in phenol conversion may include the leaching of Pd and decreased accessibility of the catalytic surface of Pd NPs due to aggregation/agglomeration of Pd NPs. To examine

DOI: 10.1021/acscatal.5b00380
ACS Catal. 2015, 5, 4121−4129

Scheme 3. Distinct Chemical Environment Surrounding the Pd NPs in Pd@sMMT-1 and Pd@rMMT-1

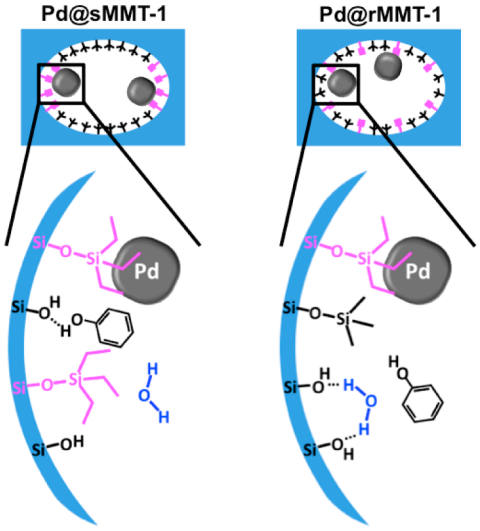

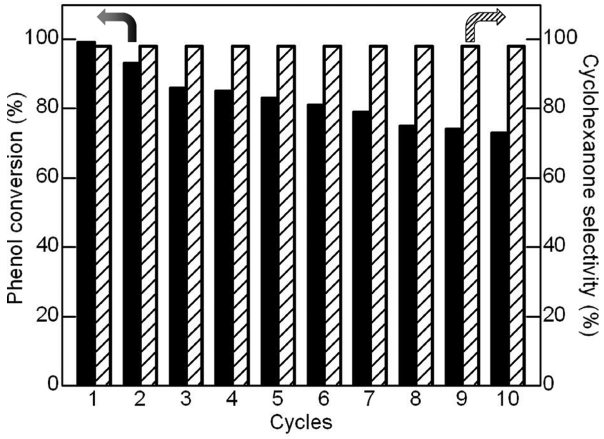

Figure 4. Reuses of Pd@sMMT-1 catalyst in the aqueous-phase phenol hydrogenation. The reaction was carried out using phenol (0.5 mmol), Pd@sMMT-1 (1.5 mol % Pd), and H_2O (2.0 mL) in H_2 (1 atm) at 25 °C for 15 h.

possible Pd leaching, the catalyst was filtered after the first, fourth, seventh, and tenth runs of reaction and the filtrates were analyzed by ICP-MS. An extremely low Pd-leachings of 0.2, 1.8, 24.4, and 49.3 ppb were detected, respectively. Even though the level of leaching was increased after successive runs, the values were still much lower than the leaching level reported for the Pd catalysts with nitrogen-containing supports under similar reaction conditions[27,28] and could contribute very little to the decreased catalyst activity. The low Pd-leaching of Pd@sMMT-1 might be associated with the hydrophobic environment surrounding Pd NPs that may prevent the ionic Pd species formed during the catalytic cycle to diffuse out of the host silica. On the other hand, the agglomeration of Pd NPs indeed took place inside the channels of MMT-1 after ten catalytic runs as indicated by wide-angle PXRD and STEM (Figure 5). The average size of Pd NPs in the ten-time reused catalyst is around 2.7 nm, as calculated from 100 particles observed in the STEM-HAADF images. The lattice fringe corresponding to the Pd(111) planes can be clearly observed (Figure 5d). The results suggested that the agglomeration of Pd NPs should be

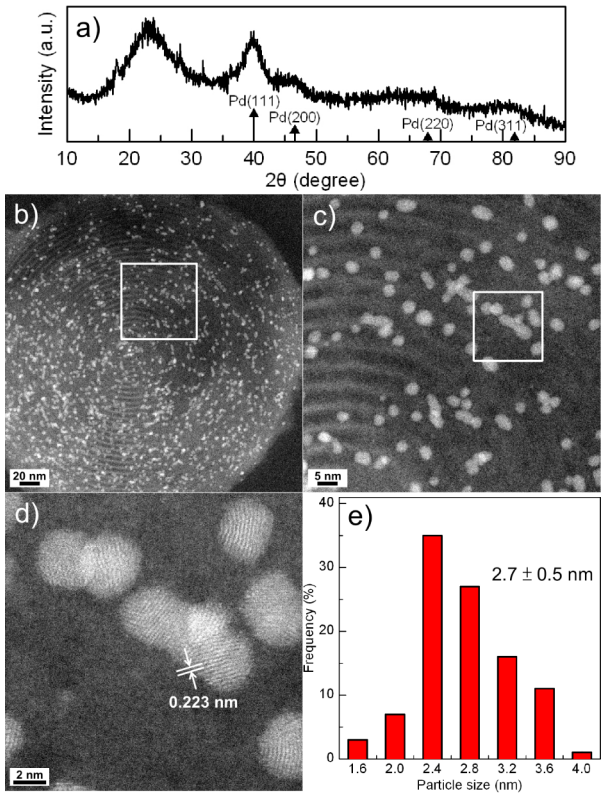

Figure 5. Wide-angle PXRD pattern (a), STEM-HAADF images (b–d), and Pd particle size distribution (e) of Pd@sMMT-1 after ten successive catalytic runs.

the main cause for the decreased catalytic activity after successive uses.

With excellent catalytic activity for the hydrogenation of phenol, Pd@sMMT-1 was further examined and applied for the aqueous-phase hydrogenation of some mono- and dihydroxylated aromatic compounds. Table 2 summarizes the substrates studied, reaction conditions, and the results obtained. Cresols were mainly converted at room temperature to the corresponding methylcyclohexanones with excellent selectivities (entries 1 and 2), but the conversion of *p*-cresol (73%) was significantly higher than that of *o*-cresol (42%). This may be due to the steric hindrance effect of the methyl group in *o*-cresol on the hydrogen bonding between the hydroxyl group of the molecule and the silanol groups on the mesopores of host silica. For *p*-chlorophenol, only dechlorination products were observed (entry 3). Cyclohexanone, a product of reductive dechlorination, was the major product of the reaction and phenol was the main side product. Such reductive dechlorination of *p*-chlorophenol to cyclohexanone has been observed by Chen et al. during the Pd-catalyzed hydrogenation in the presence of a strong acid (phosphotungstic acid) under 0.2 MPa of H_2 at 80 °C.[25] On the other hand, the Pd@sMMT-1-catalyzed hydrogenation of dihydroxyl compounds such as hydroquinone (at 25 °C, entry 4) and pyrocatechol (at 45 °C, entry 5) yielded the valuable hydroxylcyclohexanones with high selectivities and cyclohexanediols, cyclohexanone, and cyclohexanol as byproducts. For the hydrogenation of pyrocatechol, the conversion could be enhanced from 82% to ~99% by increasing the reaction temperature from 45 to 65 °C (entry 6), but the main product became *o*-cyclohexanediol and the selectivity of hydroxylcyclohexanones dropped dramatically to

DOI: 10.1021/acscatal.5b00380
ACS Catal. 2015, 5, 4121–4129

Table 2. Aqueous-Phase Hydrogenation of Hydroxyl Aromatic Derivatives with Pd@sMMT-1[a]

Entry	Substrate	T (°C)	Conversion (%)	Product selectivity (%)							
1	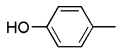	25	73	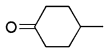	99	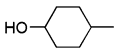	1				
2		25	42		97		3				
3	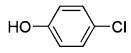	25	>99		26				72		2
4	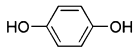	25	>99	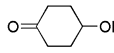	67	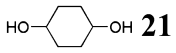	21		6		6
5		45	82		84		8		8		
6		65	>99		9		85		4	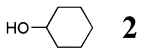	2
7	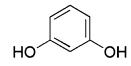	25	>99	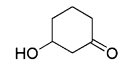	18				71	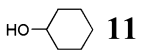	11

[a]The reactions were carried out using a substrate (0.5 mmol), Pd@sMMT-1 (1.5 mol % of Pd relative to substrate), and water (2.0 mL) in H_2 (1 atm) at 25−65 °C for 15 h.

9%. In the case of resorcinol, the main product was not hydroxylcyclohexanone but the reductive dehydration product cyclohexanone (entry 7). Similar results were observed by Antonietti and co-workers using mesoporous graphitic carbon nitride-supported Pd NPs in water under 1 bar of H_2 at 60 °C.[24] Our studies clearly show the uniqueness of Pd@sMMT-1 with purely hydrocarbon-containing (free from nitrogen or other heteroatoms) groups surrounding Pd NPs. The efficient, recyclable and "green" catalytic system is predicted to be active for the hydrogenation of other phenol derivatives, and work focused on more detailed catalytic studies is in progress.

4. CONCLUSIONS

We have designed and prepared a novel Pd catalyst supported on dually and selectively functionalized mesoporous MMT-1 silica NPs. The catalyst contains small Pd NPs surrounded by unevenly distributed hydrocarbon-containing organic groups and isolated silanol groups on mesopore surface. The catalyst exhibited superior activity for the aqueous-phase hydrogenation of phenol to produce cyclohexanone at room temperature under atmospheric pressure of hydrogen. It was also active for the aqueous-phase hydrogenation of a variety of mono- and dihydroxylated aromatic compounds.

■ ASSOCIATED CONTENT

Ⓢ Supporting Information

The Supporting Information is available free of charge on the ACS Publications website at DOI: 10.1021/acscatal.5b00380.

NMR spectra, XPS spectra, EXAFS spectrum, PXRD patterns, and STEM-HAADF image of selected samples (PDF)

■ AUTHOR INFORMATION

Corresponding Author

*Fax: 886-3-5165521. Tel.: 886-3-5731282. E-mail: cmyang@mx.nthu.edu.tw.

Author Contributions

C.J.L. prepared and characterized the samples and performed all the catalytic studies. S.H.H. assisted C.J.L. in catalytic studies. N.C.L. helped C.J.L. in sample preparation. C.M.Y. conceived of the idea of this study, supervised the work, and wrote the manuscript.

Notes

The authors declare no competing financial interest.

■ ACKNOWLEDGMENTS

We acknowledge Professor Ming-Wen Chu for the assistance in HAADF-STEM and Dr. Jyh-Fu Lee for the help in XAS measurements. This work is supported by Frontier Research Center on Fundamental and Applied Sciences of Matters (NTHU) and the Ministry of Science and Technology of Taiwan under contract no. NSC101-2628-M-007-001-MY2.

■ REFERENCES

(1) Dodgson, I.; Griffin, K.; Barberis, G.; Pignataro, F.; Tauszik, G. *Chem. Ind.* **1989**, 830−833.

(2) *World Nylon 6 and 66 Supply/Demand Report*; PCI fibers and raw Materials: Seaford, UK, 1998.

(3) Musser, M. T. Cyclohexanol and Cyclohexanone. In *Ullmann's Encyclopedia of Industrial Chemistry*; Wiley-VCH Verlag GmbH & Co. KGaA: 2000.

(4) Schuchardt, U.; Cardoso, D.; Sercheli, R.; Pereira, R.; da Cruz, R. S.; Guerreiro, M. C.; Mandelli, D.; Spinacé, E. V.; Pires, E. L. *Appl. Catal., A* **2001**, *211*, 1−17.

(5) Silva, T. F. S.; Mishra, G. S.; Guedes da Silva, M. F.; Wanke, R.; Martins, L. M. D. R. S.; Pombeiro, A. J. L. *Dalton Trans.* **2009**, 9207−9215.

(6) Wang, Y.; Zhang, J.; Wang, X.; Antonietti, M.; Li, H. *Angew. Chem., Int. Ed.* **2010**, *49*, 3356−3359.

(7) Neri, G.; Visco, A. M.; Donato, A.; Milone, C.; Malentacchi, M.; Gubitosa, G. *Appl. Catal., A* **1994**, *110*, 49−59.

(8) Narayanan, S.; Krishna, K. *Appl. Catal., A* **1998**, *174*, 221−229.

(9) Mahata, N.; Raghavan, K. V.; Vishwanathan, V. *Appl. Catal., A* **1999**, *182*, 183−187.

(10) Claus, P.; Berndt, H.; Mohr, C.; Radnik, J.; Shin, E. J.; Keane, M. A. *J. Catal.* **2000**, *192*, 88−97.

DOI: 10.1021/acscatal.5b00380
ACS Catal. 2015, 5, 4121−4129

(11) Mahata, N.; Vishwanathan, V. *J. Catal.* **2000**, *196*, 262−270.
(12) Scirè, S.; Minicò, S.; Crisafulli, C. *Appl. Catal., A* **2002**, *235*, 21−31.
(13) Velu, S.; Kapoor, M. P.; Inagaki, S.; Suzuki, K. *Appl. Catal., A* **2003**, *245*, 317−331.
(14) Rode, C. V.; Joshi, U. D.; Sato, O.; Shirai, M. *Chem. Commun.* **2003**, 1960−1961.
(15) Shore, S. G.; Ding, E.; Park, C.; Keane, M. A. *J. Mol. Catal. A: Chem.* **2004**, *212*, 291−300.
(16) Sikhwivhilu, L. M.; Coville, N. J.; Naresh, D.; Chary, K. V. R.; Vishwanathan, V. *Appl. Catal., A* **2007**, *324*, 52−61.
(17) Li, H.; Liu, J.; Xie, S.; Qiao, M.; Dai, W.; Lu, Y.; Li, H. *Adv. Funct. Mater.* **2008**, *18*, 3235−3241.
(18) Makowski, P.; Demir Cakan, R.; Antonietti, M.; Goettmann, F.; Titirici, M. M. *Chem. Commun.* **2008**, 999−1001.
(19) Chatterjee, M.; Kawanami, H.; Sato, M.; Chatterjee, A.; Yokoyama, T.; Suzuki, T. *Adv. Synth. Catal.* **2009**, *351*, 1912−1924.
(20) Liu, H.; Jiang, T.; Han, B.; Liang, S.; Zhou, Y. *Science* **2009**, *326*, 1250−1252.
(21) Cirtiu, C. M.; Dunlop-Briere, A. F.; Moores, A. *Green Chem.* **2011**, *13*, 288−291.
(22) Liu, H.; Li, Y.; Luque, R.; Jiang, H. *Adv. Synth. Catal.* **2011**, *353*, 3107−3113.
(23) Matos, J.; Corma, A. *Appl. Catal., A* **2011**, *404*, 103−112.
(24) Wang, Y.; Yao, J.; Li, H.; Su, D.; Antonietti, M. *J. Am. Chem. Soc.* **2011**, *133*, 2362−2365.
(25) Chen, A.; Zhao, G.; Chen, J.; Chen, L.; Yu, Y. *RSC Adv.* **2013**, *3*, 4171−4175.
(26) Chen, J.; Zhang, W.; Chen, L.; Ma, L.; Gao, H.; Wang, T. *ChemPlusChem* **2013**, *78*, 142−148.
(27) Li, Y.; Xu, X.; Zhang, P.; Gong, Y.; Li, H.; Wang, Y. *RSC Adv.* **2013**, *3*, 10973−10982.
(28) Li, Z.; Liu, J.; Xia, C.; Li, F. *ACS Catal.* **2013**, *3*, 2440−2448.
(29) Xu, X.; Li, H.; Wang, Y. *ChemCatChem* **2014**, *6*, 3328−3332.
(30) Yang, X.; Yu, X.; Long, L.; Wang, T.; Ma, L.; Wu, L.; Bai, Y.; Li, X.; Liao, S. *Chem. Commun.* **2014**, *50*, 2794−2796.
(31) Zhu, J. F.; Tao, G. H.; Liu, H. Y.; He, L.; Sun, Q. H.; Liu, H. C. *Green Chem.* **2014**, *16*, 2664.
(32) Fridman, V. Z.; Davydov, A. A. *J. Catal.* **2000**, *195*, 20−30.
(33) Chase, Z. A.; Fulton, J. L.; Camaioni, D. M.; Mei, D.; Balasubramanian, M.; Pham, V. T.; Zhao, C.; Weber, R. S.; Wang, Y.; Lercher, J. A. *J. Phys. Chem. C* **2013**, *117*, 17603−17612.
(34) Yang, C. M.; Lin, C. Y.; Sakamoto, Y.; Huang, W. C.; Chang, L. L. *Chem. Commun.* **2008**, 5969−5971.
(35) Huang, W. C.; Chang, L. L.; Sakamoto, Y.; Lin, C. Y.; Lai, N. C.; Yang, C. M. *RSC Adv.* **2011**, *1*, 229−237.
(36) Huang, W. C.; Lai, N. C.; Chang, L. L.; Yang, C. M. *Microporous Mesoporous Mater.* **2012**, *151*, 411−417.
(37) Lai, N. C.; Lin, C. J.; Huang, W. C.; Yang, C. M. *Microporous Mesoporous Mater.* **2014**, *190*, 67−73.
(38) Yang, C. M.; Lin, H. A.; Zibrowius, B.; Spliethoff, B.; Schüth, F.; Liou, S. C.; Chu, M. W.; Chen, C. H. *Chem. Mater.* **2007**, *19*, 3205−3211.
(39) Liu, C. H.; Guan, Y.; Hensen, E. J. M.; Lee, J. F.; Yang, C. M. *J. Catal.* **2011**, *282*, 94−102.
(40) Huang, S. H.; Liu, C. H.; Yang, C. M. *Green Chem.* **2014**, *16*, 2706−2712.
(41) Lang, N.; Tuel, A. *Chem. Mater.* **2004**, *16*, 1961−1966.
(42) Trébosc, J.; Wiench, J. W.; Huh, S.; Lin, V. S. Y.; Pruski, M. *J. Am. Chem. Soc.* **2005**, *127*, 3057−3068.
(43) Stein, A.; Melde, B. J.; Schroden, R. C. *Adv. Mater.* **2000**, *12*, 1403−1419.
(44) Hoffmann, F.; Cornelius, M.; Morell, J.; Fröba, M. *Angew. Chem., Int. Ed.* **2006**, *45*, 3216−3251.
(45) Sen, A. *Acc. Chem. Res.* **1988**, *21*, 421−428.
(46) Jentys, A. *Phys. Chem. Chem. Phys.* **1999**, *1*, 4059−4063.
(47) Dąbrowski, A.; Podkościelny, P.; Hubicki, Z.; Barczak, M. *Chemosphere* **2005**, *58*, 1049−1070.
(48) Pera Titus, M.; El Chahal, R.; Rakotovao, V.; Daniel, C.; Miachon, S.; Dalmon, J. A. *ChemPhysChem* **2009**, *10*, 2082−2089.
(49) Yilmaz, N.; Mizukami, M.; Kurihara, K. *Langmuir* **2007**, *23*, 6070−6075.

DOI: 10.1021/acscatal.5b00380
ACS Catal. 2015, 5, 4121−4129